Optical Emission Measurements of an Inductively Coupled Argon Plasma (ICP)

Steve Jaffe[1], Stanford University, Stanford, CA. USA
Rolf Hernberg, Tampere University of Technology, Tampere, Finland

This work begins by checking for different excitation and gas temperatures in the coil region of an argon ICP. These are the first published simultaneous measurements of excitation and gas temperatures in the coil region of a large diameter (75 mm), high power (14 kW), argon ICP. In the plasma core, the measured bound and free electron populations are in equilibrium at ≈ 10,000 K, while the gas temperature is only ≈2,500 K. The gas temperature rises to 8–9,000 K in a localized annulus near the plasma edge. A simplified model supports these measurements and proposes a novel structure of three concentric regions within the coil. Against the torch wall, is a narrow 'blanket annulus' of cold gas. The 'blanket annulus' surrounds a narrow 'discharge annulus' where the gas temperature is 8,500 K and the electron temperature exceeds 16,000 K. The 'discharge annulus' surrounds a broad 'photo–excited core' where kinetic temperatures are ≈2,500 K and excitation temperatures are elevated by nonlocal, resonance radiation which diffuses inward from the 'discharge annulus'.

Introduction

The ICP has applications from spectrochemical analysis to chemical vapor deposition of diamond. Optimization of these applications requires a knowledge of the electron and heavy species kinetic, i.e. translational, temperatures [1]. In atmospheric pressure ICPs, translational energies are typically Maxwell–Boltzmann distributed, and populations of excited, bound and free electronic states are typically Boltzmann distributed. While each of these distributions are respectively characterized by electron, gas, and excitation temperatures, these temperatures may not be equal. Simultaneous measurement of kinetic and excitation temperatures are rare, yet they invariably indicate

---

[1]Present address: Norton Diamond Film, c/o Technion, 14 Mason St., Irvine, CA. 92718, USA.

excitation temperatures in the range $8{,}000 \le T_{ex} \le 11{,}000$ K with T_e greater than T_{ex} and T_{gas} substantially less than T_{ex} [2-8]. The apparent lack of simultaneous excitation and kinetic temperature measurements in the coil region of a high power, argon ICP prompted the present work.

We investigate a swirl stabilized, convection cooled ICP located at the Tampere University of Technology; it provides optical access to the rf coil region. The 7.5 cm i.d. torch couples 13.8 kW at 2 MHz into 4.3 gm/sec of atmospheric pressure argon. The flow at the coil entrance is turbulent based on a calculated axial velocity of 55 m/s and a peak azimuthal velocity of 25 m/s. Across the four turn rf coil the voltage is 2 kV. We employ a suite of emission measurements: argon line emission, continuum emission and hydrogen Stark broadening, for bound and free electronic state populations, plus CN ro–vibronic emission, for heavy species kinetic temperature. Bright emission from the CN molecule allows rotational temperature measurements with impurity levels in argon of less than 0.16% N_2 and less than 0.14% CH_4 by volume. These low impurity levels do not alter argon line and continuum emission so modeling is simplified and comparison can be made with the pure argon ICP literature [9, 10]. A side benefit of methane addition is the hydrogen for Stark broadening measurements allowing redundant determination of electron density by H_β and continuum emission.

Measurement Results

Stark broadening and argon continuum (430 nm) measurements of electron density agree, with densities ranging in the coil region from 2–14 X 10^{15} cm^{-3}. The bound electronic states of argon have the same spatial distribution as the free electrons, broadly distributed over the central core region of ICP. By contrast excited CN is only found in a narrow annulus at the edge of the plasma. Measured emission intensity is converted first to volumetric emission via Abel inversion and then to excited state densities, n_k. Equations (1-3) define several excitation temperatures which are determined from free and bound electronic density measurements,

$$\frac{n_e n_i}{n_m} = \frac{2Z_1}{g_m}\left[\frac{2\pi m_e kT_{SAHA}}{h^2}\right]^{3/2} \exp\left[-\frac{E_i - E_m}{kT_{SAHA}}\right], \quad (1)$$

$$\frac{n_k}{n_m} = \frac{g_k}{g_m}\exp\left(-\frac{E_k - E_m}{kT_{ex\beta}}\right), \quad (2)$$

$$\frac{n_k}{n_a} = \frac{g_k}{Z}\exp\left(-\frac{E_k}{kT_{LTE}}\right); \quad n_a \approx p/\left(kT_{LTE}\right). \quad (3)$$

In addition, rotational temperature is determined from a simulation of the CN $B^2\Sigma^+ \rightarrow X^2\Sigma^+$, v(0,0) band fitted to several unresolved line measurements within this band. Fig. 1 shows the profiles of measured electronic excitation temperatures and the CN rotational temperature.

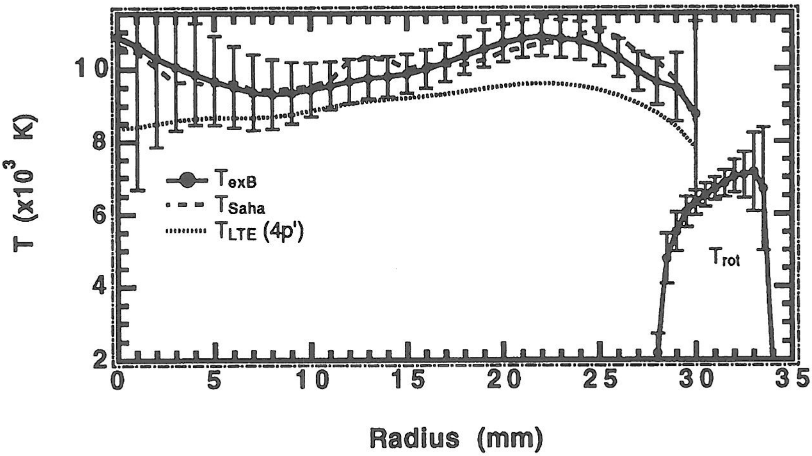

Fig. 1. Temperature results measured at the vertical midsection of the rf coil.

Throughout the coil, excitation temperatures are related by $T_{LTE}<T_{ex\beta}\approx T_{Saha}$. This relationship indicates partial local thermodynamic equilibrium (PLTE) among excited states, typical of ICP excitation temperature measurements [Owano *et al* 1990]. All of these excited state energies are approximately 15 times larger than kinetic energies, raising doubts about the coupling between excitation and kinetic temperatures. In fact, the gas temperature is too low to measure (≈2,000 K) in the center of the torch where the excitation temperatures are about 10,000 K. Near the torch wall the gas temperature is peaked in a narrow annulus. With increasing residence time in the coil, the excitation temperature profiles are largely unchanged, while the gas temperature annulus increases in height and breadth.

Model

These measurement results beg the question, "If kinetic temperatures are low in the core where excitation temperatures are high, where is the excitation source?" To locate this source we solve the electron energy equation, balancing joule heating with electron–heavy elastic collisional energy transfer,

$$T_e - T_g = \frac{m_g e^2 E_{rms}^2}{3k(m_e \nu_{e-H})^2} \quad (4)$$

The azimuthal field magnitude is estimate as 900 V/m from Faraday's law and the rf coil voltage measurement. The electric field, *E*, is assumed constant with radius, but ion and neutral densities vary greatly with radius. Where the gas temperature is elevated, the electron–heavy collision frequency, ν_{e-H}, is low. The reduced field, *E/n*, is correspondingly high — producing an annular electric discharge where Fig. 2 shows the calculated electron temperature exceeds 16,000 K.

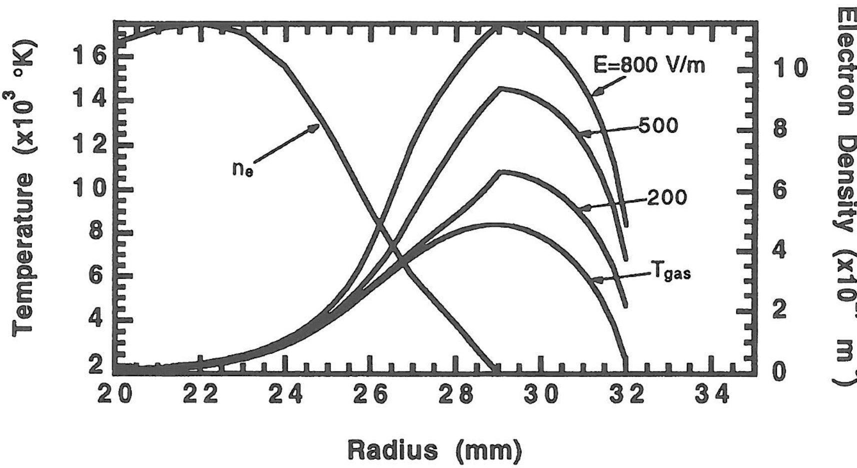

Fig. 2. Calculated electron temperature with assumed electric field strengths. Note that the abscissa scale begins at *r*=20 mm.

To see how this localized annulus of hot electrons can affect the excitation temperatures in the plasma core, we solve the steady state continuity equation for a two level model [11],

$$0 \approx \dot{n}_2(\mathbf{r}) = [\dot{n}_2(\mathbf{r})]_{\text{collisons}} - A n_2(\mathbf{r}) + A \int_{V'} n_2(\mathbf{r}') G(\mathbf{r} - \mathbf{r}') dV' \quad (5)$$

In this model all excited states, n_2, are represented by the $4s^1P_1$ state of argon. Equation (5) balances net collisional excitation with net radiative de-excitation. G(r-r') is the probability that a resonance photon emitted within *dV'* will be absorbed at r, and *A* is the radiative transition probability. Fig. 3 shows (left to right) collisional rates by thermal electron impact excitation and de-excitation, excitation by super hot electrons, n_{e*}, and quenching of n_{e*}. Note that de-excitation by a thermal electron produces $e*$ with 11.8 eV. This super hot electron goes on to re-excite through inelastic collisions with ground state atoms, n_1, or quench through elastic collisions. The net effect of n_{e*} is to reduce the collisional de-excitation rate far below the radiative de-excitation rate. The collisional excitation rate is $[\dot{n}_2]_{\text{collisions}} = 10^{26}\,\text{m}^{-3}\,\text{sec}^{-1}$ only in the inner one millimeter of the discharge annulus where both electron density and temperature are high. Elsewhere, resonance radiation, generated in the discharge annulus, produces excited states.

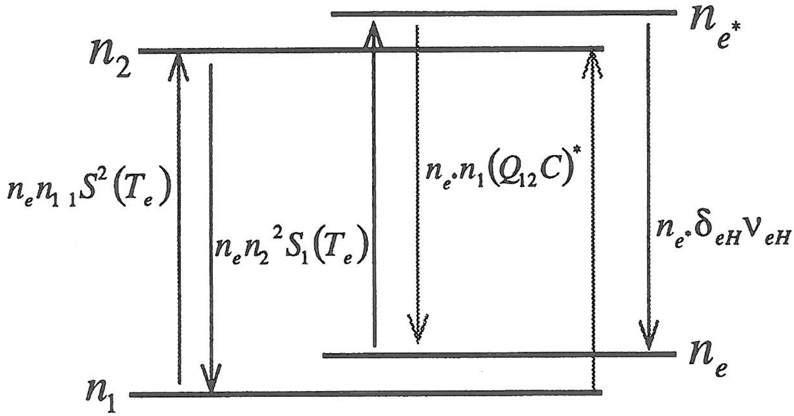

Fig. 3. Two level model of collisions. Relative energies are schematically represented by vertical position.

The dominance of radiative de-excitation and the localization of collisional excitation suggest a simplified solution of (5) based on the photon balance of Fig. 4. Here the geometry is simplified to a photo-excited core surrounded by a thin, collisionally excited annulus. Assuming the annulus is optically thin, the probability that a photon emitted in annulus enters the core is

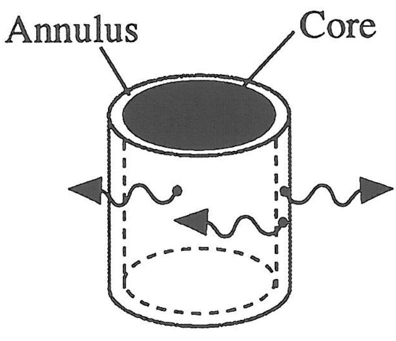

Fig. 4. Simplified radiation model.

$$\theta_{\text{annulus}} \equiv \frac{\int \Gamma_{\text{photon}}\, ds}{A \int_{\text{annulus}} n_2\, dV} = \frac{\int \Gamma_{\text{photon}}\, ds}{\int_{\text{annulus}} [\dot{n}_2]_{\text{collisions}}\, dV} = 0.5. \qquad (6)$$

Treating the core as an infinite, uniformly populated cylinder, optically thick for resonance broadened radiation, the photon escape probability from the core is calculated as [11]

$$\theta_{\text{core}} \equiv \frac{\int \Gamma_{\text{photon}}\, ds}{A \int_{\text{core}} n_2\, dV} = 2.6 \times 10^{-4}. \tag{7}$$

To evaluate the uniform density n_2 we equate the numerators of (6) & (7). Using measured dimensions of a core radius of 28 mm, an annulus i.d. of 28 mm and an o.d. of 29 mm with a mean excitation rate of 10^{26} m^{-3} sec^{-1} and a transition probability of $5X10^8$ sec^{-1}, the result is $n_2=3X10^{19}$ m^{-3}; the corresponding LTE temperature from (3) is 12,000 K. This population and temperature are slightly higher than measured, perhaps due to assumptions of infinite length or an optically thin annulus. Nevertheless, they demonstrate that radiative pumping from the discharge annulus can sufficiently photo-excite the core to generate measured excitation temperatures. This structure provides a new basis for interpreting differences between excitation and kinetic temperatures and highlights the importance of the discharge annulus to understanding ICP physics.

References

1. Kruger, C.H., Plasma Chem. and Plasma Proc., Vol.9, No.4, p.435-443, 1989
2. Baldwin, S.K., T.G. Owano, and C.H. Kruger, Plasma Chem. and Plasma Proc., Vol. 14, No. 4, p.383, December, 1994
3. Baer, D.S., Ph.D. Thesis, Stanford University, March 1993
4. Britske, M.E., V.P. Ignatko, Yu. S. Sukach, Teplofizika Vysokikh Temperature, Vol. 10, No.2, pp.265-272, March-April, 1972
5. Dresvin, S.V. and V.S. Klubnikin, Teplofizika Vysokikh Temperatur, Vol. 9, No. 3, pp.475-482, May-June, 1971.
6. Kleinmann, I. and J. Cajko, , Spectrochimica Acta, Vol 25B, p657, 1970
7. Marshall, K.A., and G.M. Hieftje, , Spectrochimica Acta., Vol.43B, Nos.6/7, p.841, 1988
8. Pei-Qi, L., G. Pei-Zhong, L. Tie-Zheng, and R.S. Houk, Spectrochimica Acta. Vol. 43B, No.3, p273, 1988.
9. Goldfarb, V.M. and H.V. Goldfarb, Spectrochimica Acta. Vol 40B, Nos. 1/2, p177, 1985
10. Gordon, M.H., Plasma Chem. and Plasma Proc., Vol.13, No.3, 1993, p.365-378
11. Irons, F.E., J.Q.R.S.T., Vol. 22, p.1, 1979